Subpicosecond Solvation Relaxation of 4-(Dicyanomethylene)-2-methyl-6-(*p*-(dimethylamino)styryl)-4*H*-pyran in Polar Liquids

P. van der Meulen, H. Zhang, A. M. Jonkman, and M. Glasbeek*

Laboratory for Physical Chemistry, University of Amsterdam, Nieuwe Achtergracht 127, 1018 WS Amsterdam, The Netherlands

Received: October 4, 1995; In Final Form: January 5, 1996[⊗]

The solvation dynamics of 4-(dicyanomethylene)-2-methyl-6-(*p*-(dimethylamino)styryl)-4*H*-pyran (DCM), dissolved in a polar solvent methanol, ethylene glycol, ethyl acetate, or acetonitrile, has been studied using the fluorescent up-conversion technique with a time resolution of ≈100 fs. Typically a bimodal dynamic Stokes shift behavior is found, with time constants of about 100 fs and a few picoseconds, respectively. The initial component in the solvation relaxation is attributed to the effect of free streaming motions of the solvent molecules, whereas the second component is typical of the rotational diffusion motions of the solvent molecules. From the initial rapid rise in the integrated emission intensity it is concluded that electron transfer is preferably to a higher lying (less emissive) charge transfer state which is formed in less than 100 fs.

1. Introduction

Solvation dynamics is a topic of considerable current interest (for reviews, see refs 1−5). In part this interest stems from the dominant role of solvation processes in the temporal evolution of a large number of chemical reactions in liquid solution.[6] Many experimental studies of solvation dynamics using time-resolved emission- or absorption-spectroscopy have been reported recently.[7] In most experiments, ultrashort laser pulses are applied to excite the solute molecules to a state in which the electronic charge distribution differs appreciably from that of the ground state. On account of the electrostatic interactions of the solute molecules with the environment, a spontaneous rearrangement of the dipolar solvent molecules surrounding the solute molecules ensues. Normally, the reorientational motions of the solvent molecules are not fast enough to adiabatically follow the laser-induced sudden changes of the electronic charges at the solute molecules. The usual time scale for the new dynamical equilibrium situation to be reached extends from tens of femtoseconds up to the picosecond regime.

When the excited state of the solute is emissive (as considered in this work), the temporal behavior of solvation relaxation might be investigated by the measurement of the dynamic Stokes shift of the emission. Several kinds of pump−probe experiments have been developed to measure the dynamic Stokes shift in the (sub)picosecond regime; we mention stimulated emission, transient absorption, and fluorescent up-conversion methods.[8] Especially the fluorescent up-conversion method is attractive because it directly monitors the temporal behavior of only the population in the emissive state undergoing the solvation relaxation (and thus the results are not influenced by the time evolution of the population in the ground state of the optical transition).

A molecular system for which the solvation dynamics has recently attracted much interest is the laser dye DCM (4-(dicyanomethylene)-2-methyl-6-(*p*-(dimethylamino)styryl)-4*H*-pyran).[9−15] The fluorescent state of DCM shows an appreciable static Stokes shift. For example, in methanol, the band maxima in the absorption and emission spectra are at about 465 and 630 nm, respectively.[9,10] The fluorescent state is characterized by a large dipole moment (26.3 D [9]) as is typical of a charge transfer state. By means of time-resolved stimulated emission decay experiments, it was demonstrated that the fluorescence of DCM in polar solutions contains transient components on a picosecond time scale.[11] The transients were discussed to be representative of the solvation dynamics occurring in the emissive charge transfer state. In a previous paper[12] we reported on fluorescent up-conversion experiments performed for DCM. It was concluded that a substantial fraction of the intramolecular charge separation (≥70%) is completed within 300 fs of the pulsed excitation. The picosecond components in the up-conversion signals were also attributed to the effects of solvation dynamics. In time-resolved transient absorption studies of DCM in methanol similar results were obtained.[14,15] In addition, the latter data yielded a temporal isosbestic point in the net gain spectra within a few picoseconds after excitation. This point showed a red shift when the polarity of the solvent was increased. It was concluded that the charge transfer state is formed within 30 ps and that the initial decay is dominated by solvation relaxation dynamics of the system. Very recently, fluorescence up-conversion experiments for DCM dissolved in the solvents methanol and chloroform were reported,[16] showing that the (sub)picosecond transients are observed only in the polar methanol solvent. It was concluded that the time-resolved transients are representative of solvation dynamics only and not of ultrafast intramolecular relaxation processes. In addition, a narrowing of the emission band on a picosecond time scale was found, and it was invoked that vibrational cooling could be involved in this narrowing process.

Here, we report on results from fluorescence up-conversion experiments for DCM dissolved in different polar solvents with a time resolution of approximately 100 fs. Part of the results has been presented recently.[17] We report that by far the larger part of the DCM solvation relaxation has taken place within a few hundred femtoseconds. Furthermore, it is reported that the solvation of DCM in fact shows bimodal character, the fastest decay component of which is representative of relaxation caused by inertial free streaming motions of the solvent molecules. In addition, we report on a rapid initial increase (on a time scale of 300 fs) in the integrated intensity of the DCM emission. It is proposed that this rapid intensity component originates from subpicosecond intramolecular relaxation from higher lying states, possibly pertaining to a slightly different molecular configuration.

[⊗] Abstract published in *Advance ACS Abstracts,* March 1, 1996.

0022-3654/96/20100-5367$12.00/0

2. Experimental Section

DCM was purchased from Exciton and dissolved without further purification. Solutions of DCM in methanol (Merck UVASOL), ethylene glycol (Aldrich), ethyl acetate (Merck UVASOL), or acetonitrile (Merck UVASOL) were prepared. The solvents were used as purchased. The concentration in each solution was approximately 10^{-4} M, as determined from the extinction in the absorption spectra. The steady-state fluorescence spectra of DCM in the various solutions (10^{-6} M) were measured using a calibrated emission spectrometer outfitted with time-correlated single-photon counting detection.[18] Solvation dynamics was studied at ambient temperatures using the time-resolved fluorescence up-conversion technique.[19] To this end, an all-line continuous wave (cw) Ar^+ laser (Coherent Innova 310) was used to pump a femtosecond Tsunami Ti:sapphire laser (82 MHz). The pulses were led through a 1 mm thick BBO frequency doubling crystal after which the pulses were split by a dichroic beam splitter into two beams, the first beam being the pump beam (at a wavelength of 420 nm, i.e., about 45 nm to the blue of the DCM absorption maximum) and the second beam being the gating beam (at 840 nm). The optical path lengths of the excitation pulses and the gating pulses could be varied independently by means of variable optical delay lines. Pulses with a duration of about 80 fs (fwhm supposing a $sech^2$ pulse shape) and an energy of about 1 nJ/pulse were used to photoexcite the DCM solution. The latter was contained in a flow cell of 1 mm thickness. The gating beam passed a stepping motor-driven translational stage (Micro Control, minimum step length is 0.6 fs) and was focused together with the pump-beam induced DCM fluorescence onto a 1 mm thick BBO crystal. The up-conversion signal (at a frequency equal to the sum of the frequencies of the fluorescence and the Ti:sapphire fundamental frequency, i.e., in the wavelength range between 320 nm and 380 nm) was filtered by an UG11 filter and focused by means of a lens on the entrance slit of the monochromator (Zeiss M 20, spectral resolution < 5 nm). To circumvent contributions to the probed fluorescence transients arising from reorientational motions of the probe, the transients were measured under magic angle conditions; i.e., the polarization of the excitation beam was rotated at the magic angle of 54° 44 min with respect to the vertically polarized gating beam. To this end, a quartz polarizer controlling the polarization of the pump beam was placed in the pump arm. Photodetection was by means of a photomultiplier (EMI 9863 QB/350) connected to a photon-counting system (PAR 1120/1109). For each delay time, the up-conversion signal was accumulated for 1 s. A schematic view of the experimental setup is presented in Figure 1. The instrumental response function as deduced from the measured cross correlation function of the excitation and the gating pulses (at 420 and 840 nm, respectively) was determined to be ≈ 150 fs (fwhm). Transients were recorded using "short" and "long" time windows of 3.3 and 33 ps, respectively. A personal computer was used for data acquisition, storage, and analysis.

3. Results

Representative fluorescent transients as observed at a few detection wavelengths for a 10^{-4} M solution of DCM in ethylene glycol following pulsed laser excitation at 420 nm are presented in Figure 2. Analogous results were obtained for DCM dissolved in the other solvents. Previously, fluorescence transient decay data were presented for DCM in methanol.[12] It should be added, however, that in the current experiments a flow cell and low-energy laser pulses were used and that special care was taken to avoid warming of the solution. The data of Figure 2 are typical of what is observed for all solutions studied in this paper. The emission transients detected in the blue region of the fluorescence spectrum are characterized by an instantaneous rise and picosecond decay components. When detection is more to the red, however, the decay part slows down until eventually an initial rise on a picosecond time scale is observed. These overall features are in agreement with results previously reported elsewhere[12] and are well-recognized as being characteristic of the solvation taking place in DCM in its emissive charge transfer state.

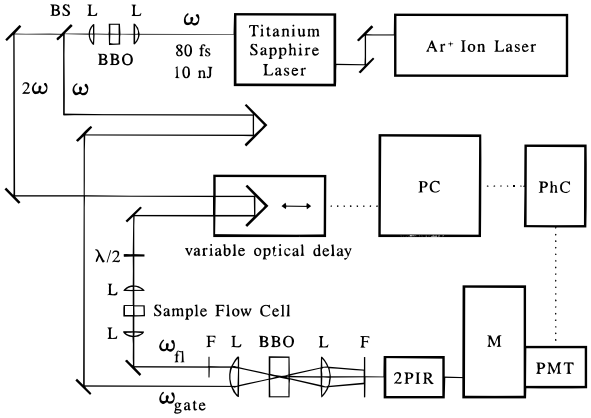

Figure 1. Schematic view of the experimental setup: L, lens; BBO, β-barium borate nonlinear optical crystal; BS, dichroic beam splitter; $\lambda/2$, half wave plate; F, filter; 2PIR, 2-prism image rotator which transfers directional variations of the up-converted fluorescence beam in the horizontal plane to directional variations in the vertical plane; M, monochromator; PMT, photomultiplier tube; PhC, photon counting system; PC, personal computer.

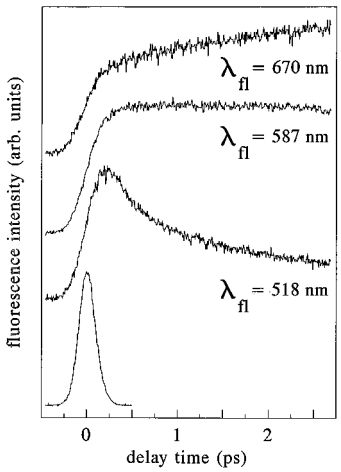

Figure 2. Representative fluorescence up-conversion transients of DCM dissolved in ethylene glycol recorded at 320, 345, and 370 nm, corresponding to fluorescence emitted at 518, 587, and 670 nm, respectively. The experimental response function, obtained from a cross-correlation of the excitation and gating beams, is shown in the lower left corner.

To construct the spectra at various times, *t*, following the excitation pulse, we have adopted the method of Maroncelli and Fleming.[20] First, for every solution the fluorescent transients were measured as a function of detection wavelength in the range from 520 up to 695 nm, in intervals of around 15 nm. The observed fluorescent transients were fit to a function which is the convolution of the instrumental response function with a sum of four exponentials using a nonlinear least squares fitting procedure.[21] The purpose of this fitting is to obtain the decays in an analytic form suitable for further data analysis, and at this stage no physical meaning should be attached to the parameters of the exponential functions. For each detection wavelength, the time-integrated fluorescence decay transient was

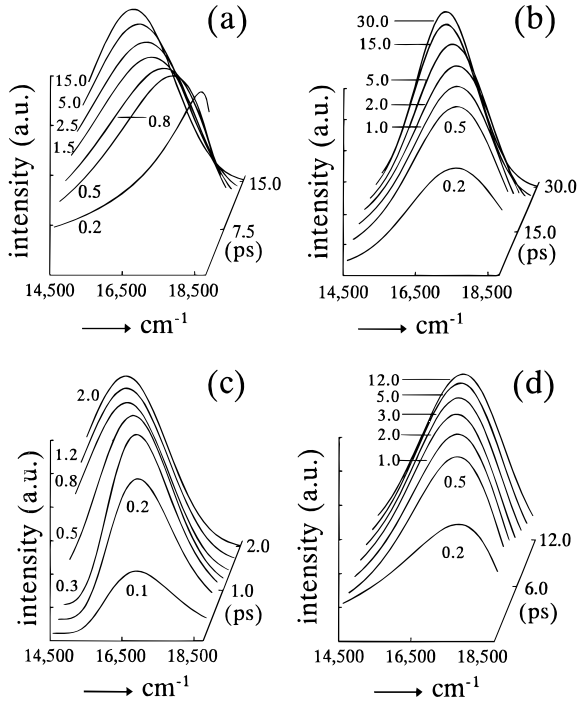

Figure 3. Log-normal fits to the reconstructed fluorescence spectra of DCM dissolved in (a) methanol, (b) ethylene glycol, (c) acetonitrile, and (d) ethyl acetate.

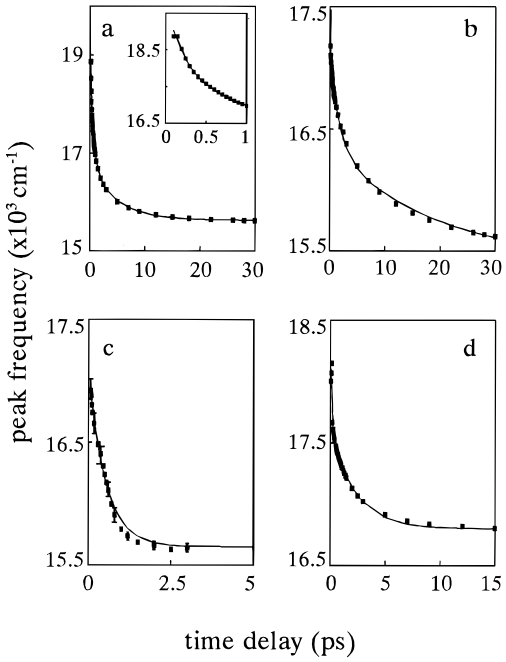

Figure 4. Time evolution of the peak frequency of DCM dissolved in (a) methanol, (b) ethylene glycol, (c) acetonitrile, and (d) ethyl acetate. Experimental data points are drawn as squares, whereas the results of the fits according to eq 3 are represented by full curves. Some representative error bars are shown.

normalized to the intensity at that wavelength of the calibrated steady-state emission spectrum. The fluorescence intensity at time t as discerned from the deconvoluted transients at the series of detection wavelengths was plotted versus the detection wavelength. The resulting time-resolved spectra were transposed to a wave number scale and fitted with a log-normal shape function,[20]

$$f(\nu) = \begin{cases} g_0 \exp\left\{\ln(2)\left(\dfrac{\ln[1+2b(\nu-\nu_p)/\Delta]}{b}\right)^2\right\} & \text{if } 2b(\nu-\nu_p)/\Delta > -1 \\ 0 & \text{else} \end{cases} \quad (1)$$

In eq 1, Δ is the bandwidth, b is the asymmetry parameter, and ν_p is the frequency of the band maximum. Figure 3 displays the time-resolved spectra thus obtained for DCM in the various solutions. As can be seen from Figure 3a, the band maximum in the emission spectrum for DCM in methanol shifts from 18.5 kK at about 200 fs after the pulsed excitation to 15.5 kK about 30 ps after the preparation pulse. Similar results were obtained when DCM was dissolved in ethylene glycol, acetonitrile, and ethyl acetate. The data are collected in Figures 3b−d. For all solutions the broad band emission (typical of the charge transfer character of the emissive state) showed an appreciable dynamic Stokes shift. Also, for all solutions the trailing edge of the solvation dynamics takes place on the picosecond time scale.

4. Discussion

The dynamic Stokes shift can be represented by either the time-dependence of the peak frequency ($\nu_p(t)$) or the first moment ($\bar{\nu}(t)$) of the log-normal fit emission spectrum. Very recently,[22] it has been discussed that in the case of coumarine 153 there is very little difference for the time behavior due to solvation of the two parameters, $\nu_p(t)$ and $\bar{\nu}(t)$. However, for the DCM solutions investigated here we found that the scatter in the simulated spectra, especially at the earliest times after excitation, caused a higher uncertainty in $\bar{\nu}(t)$ than in $\nu_p(t)$. For this reason in the following we restrict ourselves to the discussion of the temporal data obtained for $\nu_p(t)$. In Figure 4 we depict $\nu_p(t)$ as a function of t as deduced from the log-normal fits to the reconstructed emission spectra. Note that the time dependence of $\nu_p(t)$ is the same as that for the normalized spectral response function, $S_\nu(t)$, with

$$S_\nu(t) \equiv \frac{\nu(t) - \nu(\infty)}{\nu(0) - \nu(\infty)} \quad (2)$$

where it is understood that according to linear response theory the time dependence of $S_\nu(t)$ equals that of the time correlation function for the resonance frequency of the solute molecules as caused by the fluctuations in the bath of solvent molecules.[23] The reason for plotting $\nu_p(t)$ in Figure 4 rather than $S_\nu(t)$ is that on the one hand its time dependence is equal to that for $S_\nu(t)$ and on the other hand we avoid the difficulty that may arise in $S_\nu(t)$ due to the uncertainty in the frequency of the charge transfer state emission at $t = 0$.

To show more clearly the earliest time behavior of $\nu_p(t)$, we have included, as an insert, in Figure 4 for DCM in methanol, the dynamic Stokes shift behavior during the initial picosecond of the solvation process. Clearly, a bimodal solvation relaxation behavior can be inferred. We note in passing that such a bimodal behavior has recently been found also by Rosenthal et al. for the probe molecules 1-aminonaphthalene and coumarin 153, also dissolved in methanol.[24]

Recent experiments with time resolution on the order of 100 fs have revealed that the spectral response function for chemically inert polar solutes in highly polar small-molecule solvents contains ultrafast decay components with time constants on the order of a few hundred femtoseconds or faster.[2,22,24−26] The presence of the subpicosecond decay components cannot be explained satisfactorily within the context of rotational diffusion motions of the solvent molecules being responsible for the solvation relaxation process.[2] However, molecular dynamics and Brownian oscillator[27] model studies have shown that the ultrafast decay components in the spectral response function can be accounted for when contributions from inertial free

TABLE 1: Solvent Correlation Function $S_\nu(t)$[a]

solvent	a_g	ω_g (ps^{-1})	a_1	τ_1 (ps)	a_2	τ_2 (ps)	total shift[b] (cm^{-1})	τ_e[c] (ps)
methanol	0.2	6	0.5	0.7	0.3	5	3800	1
ethylene glycol	0.3	13	0.4	3	0.3	27	2400	4
acetonitrile[d]			1.0	0.5			1400	0.5
ethylacetate	0.4	7	0.6	2			1400	0.9

[a] $S_\nu(t)$ is fitted to a function of the form $S_\nu(t) = a_g \exp(-{}^1/_2\omega_g{}^2t^2) + a_1 \exp(-t/\tau_1) + a_2 \exp(-t/\tau_2)$. [b] The total shift is calculated by adding the preexponential factors obtained by fitting the *unnormalized* peak position $\nu_p(t) - \nu_p(\infty)$, instead of the *normalized* $S_\nu(t)$, to a function of the same form; $\nu_p(\infty)$ is obtained from the steady-state fluorescence spectrum. [c] τ_e is the time required for $S_\nu(t)$ to decay to $e^{-1} = 0.368$; it represents an average solvation time. [d] The solvation dynamics of acetronitrile could not be fitted with a Gaussian component. Presumably, the Gaussian component is too fast to be be detected experimentally, and only the (exponential) trailing edge of the solvation is observed.

streaming motions of the solvent molecules (small angle displacements being sufficient) are included in the considerations.[2,24−26,28] These "inertial free streaming" motions are characteristic of the rapid collisionless rotational motions of the solvent molecules in the solvent cage. Due to the inertia of the solvent molecular motions, these motions are not influenced instantaneously as the solute molecules become photoexcited.[28] On the other hand, the inertial motions affect the configurations of the solvent molecules around the solute, and it has been shown that small angle configurational changes are to a significant extent responsible for the relaxation of the free energy of solvation.[24,28] For the DCM solvation relaxation results reported here we believe that both inertial and rotational diffusion motions are relevant. For example, for DCM in methanol, the time correlation function characterizing the solvation relaxation could be fitted to a function of the form (cf. the drawn curve in Figure 4)

$$S_\nu(t) \propto a_G \exp(-{}^1/_2\omega_G{}^2t^2) + a_1 \exp(-t/\tau_1) + a_2 \exp(-t/\tau_2) \quad (3)$$

with best fit values of $a_G = 0.2$, $a_1 = 0.5$, $a_2 = 0.3$, $\omega_G = 6$ ps^{-1}, $\tau_1 = 0.7$ ps, and $\tau_2 = 5$ ps. The data obtained for DCM dissolved in the other solvents have been analyzed similarly, and the corresponding results have been collected in Table 1.

The ultrafast decay components in the solvation process in the various polar solvents with the characteristic time constant of $1.4\omega_G{}^{-1}$ of about 100 fs are compatible with the values reported recently by Rosenthal et al. for the short relaxation component found for the probe molecules 1-aminonaphthalene and coumarin 153, also dissolved in polar solvents.[24] Molecular dynamics calculations by the same authors yielded solvation time correlation functions containing a large-amplitude fast decaying component with a time constant of about 100 fs. The latter was discussed to arise to a large extent (≥50%) from inertial free streaming rotational motions of the methanol molecules (not including the still faster O−H librational motion) in the solvent cage. Very recently, the study of the solvation dynamics of the C153 probe was extended to a whole series of different solvents.[22] From their thorough study Horng et al. could confirm the presence of ultrafast relaxation components of at most a few hundred femtoseconds. Molecular dynamics calculations[29] suggest that low-frequency intramolecular modes could also contribute to the ∼100 fs solvation decay component. Our data for DCM, as represented in Table 1, indicate an appreciable contribution of about 30% of the ∼100 fs Gaussian decay component to the experimentally resolved dynamic Stokes shift. As in the case of the C153 probe molecule, we attribute this subpicosecond solvation decay component to originate from inertial motions of the solvent molecules.

Our results for τ_1 and τ_2 for DCM in methanol may be compared with the values of 3 and 15 ps, respectively, for the longest decay components of the solvation response function for C153 in methanol fitted to a multiexponential sum decay function, as recently reported by Horng et al.[22] By now it is well-recognized that rotational diffusion motions of the solvent molecules occur on a time scale of a few picoseconds.[1,2] Picosecond rotational diffusion motions have also been confirmed by molecular dynamics calculations.[2,29,30] Likewise we attribute the trailing edge of the solvation decays, characterized by the τ_1 and τ_2 decay constants of Table 1, to originate from the contribution of the rotational diffusion motions of the pure solvent to the solvation relaxation of the excited DCM molecules.

Up to now the influence of other ultrafast relaxation phenomena that in principle could affect the temporal spectral shape function have not been considered. It is recalled that excitation of DCM was near 420 nm, i.e., the vibrational excess energy is estimated to be larger than 4000 cm^{-1}.[9,10] Consequently, it may be asked to what extent intramolecular vibrational relaxation may have caused the observed fluorescence transients for DCM. For a few other rather large organic dye molecules, like Nile blue or oxazine[31] in liquid solution, it has been shown from fluorescence decay measurements on an ultrafast time scale that typical decay times for vibrational relaxation in the excited electronic state are less than 50 fs. By analogy, it is very likely that for the DCM dye molecule (for which the size is comparable) the vibrational relaxation dynamics should be on a similar time scale. It is thus believed that intramolecular vibrational relaxation is complete within the pulse duration and the observed transients are characteristic of the solvation relaxation of the solute molecules.

Of interest are the time dependences in the integrated fluorescence intensity of DCM as a function of t. In Figure 5 we present plots for $I(t)$ of DCM in the solvents methanol, ethylene glycol, acetonitrile, and ethyl acetate. In all solvents, the integrated emission intensity of DCM has decreased to about 30% of its initial value after the completion of the solvation relaxation. The time dependence of $I(t)$ leading to this decrease of the total emission intensity is readily understood considering (i) the effect of solvation relaxation on the frequency of the emission and (ii) the Einstein expression for the integrated intensity of the spontaneous emission which we take to vary as $\nu_p{}^3$. Since in the pulse-laser experiment the frequency of the emission band maximum undergoes a Stokes shift as time progresses, we expect a decrease in the total emission intensity in accordance with $\nu_p{}^3$ behavior. We have included in Figure 5 the time dependence of $\nu_p{}^3(t)$, where $\nu_p(t)$ is the frequency of the emission band maximum in the log-normal fitted spectrum (cf. Figure 2). It is clear from Figure 5 that, for $t > 1$ ps and taking into account that the estimated accuracy of the integrated intensity values is about 10%, the decay with time of the emission intensity is in reasonable agreement with the expected behavior. It thus follows from the integrated intensity data that at a time $t \sim 1$ ps and onward, the DCM emission originates in a single electronic state for which the electronic wave function is not influenced by the variation with time of the solvation coordinate.

Previously we reported a somewhat higher total intensity decrease of about 50% for DCM dissolved in methanol to result from the solvation relaxation, and since the $\nu_p{}^3$ dependence was not fully satisfied, a slight mixing with the locally excited state was conjectured (implying a residual electron transfer of about

30% after excitation of the lowest excited singlet state).[12] Most likely, sample warming might have caused the slightly higher intensity decrease (50% vs 30%), since at the time a flow cell was not yet at our disposal. However, as detailed below, our main previous conclusion, namely, that the major part of the charge separation process (≥70%) has been completed within the duration time of the exciting laser pulse in our experiment, still holds.

As also shown in Figure 5, a rapid initial rise with t is observed in the total emission intensity of DCM. This rise extends to within the first couple of picoseconds following the excitation pulse and certainly is well outside the time resolving power of the experiments. We conjecture that as the solvation has been initiated (due to the inertial solvent motions), the population of the solvating charge transfer state concurrently is replenished. This fast feeding of the charge transfer state that is being monitored (on a time scale of several hundreds of femtoseconds) probably arises from intramolecular relaxation from higher lying, but less emissive, molecular levels of DCM. Since these higher lying levels keep feeding the lowest emissive level in pace with the solvation dynamics of the latter, it is likely that the solvation behavior of these levels is similar to that of the probed lowest emissive state. The idea is borne out by a numerical calculation of the evolution with time of the population of the charge transfer state, taking into account solvation relaxation on the one hand and additonal feeding on the other hand. In the analysis, the time evolution of the probed charge transfer population is given by the following diffusion-feeding equation,[32]

$$\frac{\partial \rho_1(X,t)}{\partial t} = D_1(t)\frac{\partial}{\partial X}\left[\frac{\partial}{\partial X} + \frac{1}{k_B T}\frac{\partial V_1(X)}{\partial X}\right]\rho_1(X,t) + k_{2\rightarrow 1}(X)\,\rho_2(X,t) \quad (4)$$

$$D_1(t) = -\langle(\delta X)^2\rangle_1 \frac{\dot{S}_\nu(t)}{S_\nu(t)} \quad (5)$$

$$V_1(X) = V_1^{EQ} + \lambda_1(1-X)^2 \quad (6)$$

where $\rho_1(X,t)$ is the probability distribution in the probed charge transfer level $|1\rangle$ as a function of the solvation coordinate X and the time t, $D_1(t)$ is the time-dependent solvation polarization diffusion coefficient, $V_1(X)$ is the free energy of the system with the solute in level $|1\rangle$, k_B is the Boltzmann constant, T is the absolute temperature, $V^{EQ}{}_1$ is the equilibrium free energy of the system with the solute in level $|1\rangle$, λ_1 is the solvent reorganization energy with the solute in level $|1\rangle$, and $k_{2\rightarrow 1}(X)$ is the rate constant for the $|2\rangle \rightarrow |1\rangle$ radiationless transition. The first term on the right side of eq 4 is representative of the diffusional motion along X, whereas the last term characterizes the additional feeding from a single higher level $|2\rangle$. For the time development of $\rho_2(X,t)$ an equation similar to eq 4, but without the last term, applies.

Following ref 32, the time-dependent fluorescence spectrum was calculated according to,

$$I_{1\rightarrow 0}(\nu,t) \propto \int \mathrm{d}X\, g(\nu_0(X),\nu-\nu_0(X))\,\rho_1(X,t)\nu^3 \quad (7)$$

$$\nu_0(X) = \frac{V_1(X) - V_0(X)}{h} \quad (8)$$

$$V_0(X) = V_0^{EQ} + \lambda_0 X^2 \quad (9)$$

where ν is the emission frequency, $g(\nu_0(X), \nu - \nu_0(X))$ is a vibrational line shape function, and $\nu_0(X)$ is the energy gap between the charge transfer state $|1\rangle$ and the molecular ground state $|0\rangle$. In the present treatment level $|2\rangle$ is considered to be a "dark" state and, consequently, no contribution to the emission spectrum results from this level.

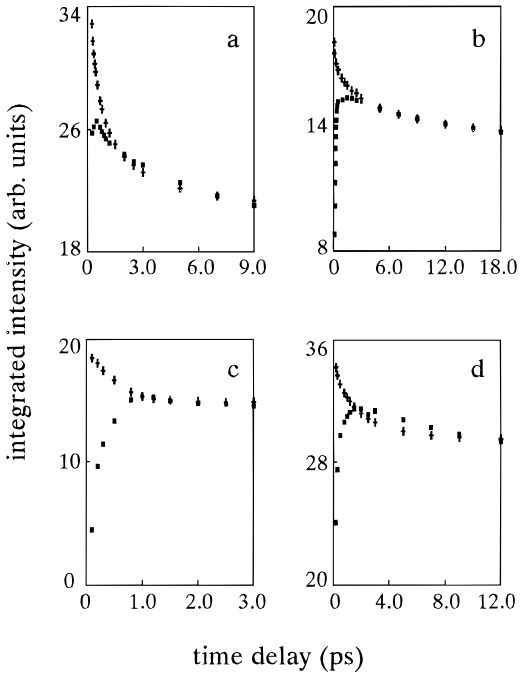

Figure 5. Time evolution of the integrated emission intensity of DCM dissolved in (a) methanol, (b) ethylene glycol, (c) acetonitrile, and (d) ethyl acetate. Experimental data points are drawn as squares. The $\nu_p{}^3$ dependence of the integrated emission intensity is represented by plus symbols.

We will illustrate the model outlined above for the case of DCM dissolved in ethylene glycol. The coupled equations for $\rho_1(X,t)$ and $\rho_2(X,t)$ were solved for the parameter values T = 295 K, $2\lambda_0 = \lambda_1 = \lambda_2 = 2200$ cm^{-1}, and $k_{2\rightarrow 1}(X) = 3$ ps^{-1}. Furthermore, it was assumed that, at $t = 0$, the equilibrium (Boltzmann) population of the ground state $|0\rangle$ was impulsively transferred to state $|2\rangle$, i.e. $\rho_1(X,0) = 0$, and $\rho_2(X,0) = \rho_0(X,0) \propto \exp(-V_0(X)/k_BT)$. The emission spectra were simulated using $\Delta V^{EQ} = V_1{}^{EQ} - V_0{}^{EQ} = 17950$ cm^{-1}. For DCM the vibrational line shape function could not readily be obtained from the emission spectrum in an apolar solvent[32] (see below), so we have chosen to represent $g(\nu_0(X),\nu-\nu_0(X))$ by a Gaussian with a full width at half-maximum of 1950 cm^{-1}. We verified that the current parameter set correctly describes the steady-state fluoresence spectrum, $I_{1\rightarrow 0}(\nu,\infty)$.

In Figure 6, a comparison is made between the experimental and simulated time evolution of the fluorescence spectrum of DCM in ethylene glycol. As can be seen from Figure 6a,b, the major experimental observables, viz., the peak position and the integrated emission intensity, are well-reproduced. With regard to the band width (Figure 6c) and the peak height (Figure 6d), the agreement is somewhat less satisfactory, but both the decrease in the peak width and the (sub)picosecond increase in the peak height are indeed qualitatively produced in the simulation.

We would like to point out that the simulation is performed with a highly simplified model. Notably, the vibrational line shape function $g(\nu_0(X),\nu-\nu_0(X))$ is approximated by a simple Gaussian. For molecules like ADMA or bianthryl,[32] quite acceptable results were obtained by equating $g(\nu_0(X),\nu-\nu_0(X))$ to the emission spectrum in the apolar solvent 3-methylpentane. In the case of DCM this approach cannot be adopted, because the emission spectrum in the very polar solvent methanol is

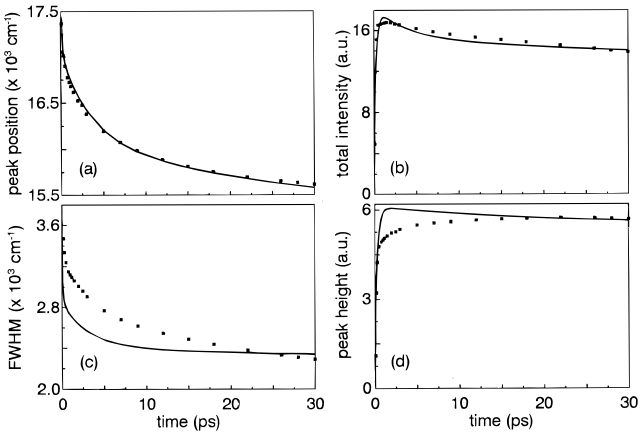

Figure 6. Time evolution of the parameters characterizing the fluorescence spectrum of DCM dissolved in ethylene glycol. The experimental results are represented by squares, whereas the results of the simulation are given by a drawn curve: (a) peak position; (b) integrated emission intensity; (c) band width (fwhm); (d) peak height.

substantially narrower than the one observed in the very apolar solvent isooctane.[10] Evidently for DCM a dependence of the vibrational line shape function on solvent polarity exists. In addition, $g(\nu_0(X),\nu-\nu_0(X))$ was assumed not to change with both X and time. Our assumption of a time-independent vibrational line shape function is consistent with the notion of ultrafast vibrational realxation discussed above, but may not be fully justified if the excited-state charge distribution, and thus the molecular force field, is changing during the solvation process, e.g., through hydrogen bonding or in the case of an electron transfer reaction in the strongly adiabatic limit.

The choice of different force constants[33] for states $|1\rangle$ and $|0\rangle$ (cf. eqs 6 and 9) is largely motivated by the observed spectral narrowing. In principle, any variation in the spectral width can be caused by a change in the vibrational line shape function, but, as remarked in the preceding paragraph, in the present simulations $g(\nu_0(X),\nu-\nu_0(X))$ is kept constant, and the spectral narrowing is attributed to the narrowing of the population distribution $\rho_1(X,t)$ induced by the higher force constant of level $|1\rangle$ compared to that of level $|0\rangle$. Considering the results of several recent molecular dynamics simulations,[34] a factor of 2 between the force constants of level $|1\rangle$ and $|0\rangle$ appears to be quite reasonable. However, it has been shown[34,35] that in case the linear response approximation breaks down, as indicated by the different force constants for the levels $|1\rangle$ and $|0\rangle$, the harmonic nature of the free energy curves is inevitably lost, and serious errors may be introduced if one continues to use these parabolic curves. Interestingly, preliminary calculations suggest that the discrepancy in Figure 6c, where the magnitude of the spectral narrowing is predicted correctly but its time dependence is calculated to be too fast, is significantly reduced if quartic free energy curves of the type introduced by Yoshimori et al.[34] are employed. At the same time, the agreement for the peak height is improved, which is easily understood since, for a given integrated emission intensity, the peak height and width are intimately related. These matters will be discussed in more detail in a forthcoming paper.[36]

In the simulations, the feeding of level $|1\rangle$ is considered to proceed via a single, dark level $|2\rangle$, which itself is impulsively populated at $t = 0$, and for which the solvation behavior is equal to that of level $|1\rangle$. This would indicate that level $|2\rangle$ either is photoexcited directly or is formed from yet another (locally excited) state within the time resolving power of the experiment. Keeping in mind that the charge transfer character of level $|2\rangle$ is similar to that of level $|1\rangle$ ($\lambda_1 = \lambda_2$), the former suggestion appears less likely on the basis of oscillator strength considerations. Hence, it is concluded that the charge separation process in DCM is completed within about 100 fs. Therefore, the laser dye DCM provides another example of a molecule for which the charge separation is much faster than the time scale for the reorientional motions of the surrounding solvent molecules. In this respect, the behavior of DCM resembles that of the betaines and mixed valence transition metal complexes[37] as well as oxazine[38] and Nile blue−DMA[39] in liquid solution.

It is interesting to note that our conclusion of an initially higher lying, excited, charge transfer state $|2\rangle$ being preferentially formed may be an illustrative example of the electron transfer mechanism recently discussed by Jortner and Bixon.[40] In particular, in the inverted regime, higher lying excited charge transfer states possess a lower barrier for electron transfer and are thus formed more rapidly. Subsequently, population relaxation of the excited charge transfer state will enhance the population of level $|1\rangle$. The latter radiationless decay process then gives rise to the additional feeding term as incorporated in eq 4.

In summary, we have studied the solvation dynamics of DCM dissolved in several polar solvents. Typically, a bimodal Stokes shift behavior is found, with time constants of about 100 fs and of several picoseconds, respectively. The initial component in the solvent relaxation is attributed to the effect of inertial free streaming motions of the solvent molecules, whereas the second component is thought to be representative of the diffusional reorientational motions of the solvent molecules. From the rapid (sub)picosecond rise of the integrated emission intensity it was concluded that the excited state electron transfer is preferentially to a higher lying, but less emissive, charge transfer state which is formed within about 100 fs and which subsequently relaxes radiationlessly on a subpicosecond time scale to a lower lying, but more emissive, charge transfer state.

Acknowledgment. This work was supported in part by the Netherlands Foundation for Chemical Research (SON) with financial aid from the Netherlands Organization for Scientific Research (NWO).

References and Notes

(1) Barbara, P. F.; Jarzeba, W. *Adv. Photochem.* **1990**, *15*, 1.
(2) Maroncelli, M. *J. Mol. Liq.* **1993**, *57*, 1.
(3) Simon, J. D. *Acc. Chem. Res.* **1988**, *21*, 128.
(4) Bagchi, B.; Chandra, A. *Adv. Chem. Phys.* **1991**, *80*, 1.
(5) Ladanyi, B.; Skaf, M. S. *Annu. Rev. Phys. Chem.* **1993**, *44*, 335.
(6) Hynes, J. T. In *Ultrafast Dynamics of Chemical Systems*; Simon, J. D., Ed.; Kluwer: Dordrecht, The Netherlands, 1993; p 345. Rossky, P. J.; Simon, J. D. *Nature* **1994**, *370*, 263. Weaver, M. J. *Chem. Rev.* **1992**, *92*, 463. Yoshihara, K.; Tominaga, K.; Nagasawa, Y. *Bull. Chem. Soc. Jpn.* **1995**, *68*, 696.
(7) For a recent review, see: *Ultrafast Phenomena IX*; Barbara, P. F., Knox, W. H., Mourou, G. A., Zewail, A. H., Eds.; Springer: Berlin, 1994.
(8) Fleming, G. R. *Chemical Applications of Ultrafast Spectroscopy*; Oxford University Press: New York, 1986.
(9) Meyer, M.; Mialocq, J. C. *Opt. Commun.* **1987**, *64*, 264.
(10) Drake, J. M.; Lesiecki, M. L.; Camaioni, D. M. *Chem. Phys. Lett.* **1985**, *113*, 530. Hsing-Kang, Z.; Ren-Lan, M.; Er-Pin, N.; Chu, G. *J. Photochem.* **1985**, *29*, 397. Meyer, M.; Mialocq, J. C.; Rougée, M. *Chem. Phys. Lett.* **1988**, *150*, 484. Meyer, M.; Mialocq, J. C.; Perly, B. *J. Phys. Chem.* **1990**, *94*, 98.
(11) Easter, D. C.; Baronavski, A. P. *Chem. Phys. Lett.* **1993**, *201*, 153.
(12) Zhang, H.; Jonkman, A. M.; Van der Meulen, P.; Glasbeek, M. *Chem. Phys. Lett.* **1994**, *224*, 551.
(13) Marguet, S.; Mialocq, J. C.; Millie, P.; Berthier, G.; Momicchioli, F. *Chem. Phys.* **1992**, *160*, 265.
(14) Mialocq, J. C.; Pommeret, S.; Naskrecki, R.; Baldacchino, G.; Gustavsson, T. *SPIE* **1994**, *2370*, 253.
(15) Martin, M. M.; Plaza, P.; Meyer, Y. H. *Chem. Phys.* **1995**, *192*, 367.
(16) Gustavsson, T.; Baldacchino, G.; Mialocq, J. C.; Pommeret, S. *Chem. Phys. Lett.* **1995**, *236*, 587.

(17) Glasbeek, M.; Jonkman, A. M.; Van der Meulen, P.; Zhang, H. *Fast Elementary Processes in Chemical and Biological Systems*; Proceedings, Lille, France, American Institute of Physics: New York, 1995.

(18) Middelhoek, E. R.; Van der Meulen, P.; Verhoeven, J. W.; Glasbeek, M. *Chem. Phys.* **1995**, *198*, 373.

(19) Kahlow, M. A.; Jarzeba, W.; DuBrull, T. P.; Barbara, P. F. *Rev. Sci. Instrum.* **1988**, *59*, 1098.

(20) Maroncelli, M.; Fleming, G. R. *J. Chem. Phys.* **1987**, *86*, 6221.

(21) Press, W. H.; Flannery, B. P.; Teukolsky, S. A.; Vetterling, W. T. *Numerical Recipes*; Cambridge University Press: Cambridge, U.K., 1986.

(22) Horng, M. L.; Gardecki, J.; Papazyan, A.; Maroncelli, M. *J. Phys. Chem.* **1995**, *99*, 17311.

(23) Kubo, R.; Toda, M.; Hashitsume, N. *Statistical Physics II*; Springer: New York, 1991.

(24) Rosenthal, S. J.; Jimenez, R.; Fleming, G. R.; Kumar, P. V.; Maroncelli, M. *J. Mol. Liq.* **1994**, *60*, 25.

(25) Maroncelli, M.; Kumar, P. V.; Papazyan, A.; Horng, M. L.; Rosenthal, S. J.; Fleming, G. R. In *Ultrafast reaction dynamics and solvent effects*; Gaudel Y., Rossky, P. J., Eds.; American Institute of Physics: New York, 1994, p 310. Jimenez, R.; Fleming, G. R.; Kumar, P. V.; Maroncelli, M. *Nature* **1994**, *369*, 471.

(26) Bingemann, D.; Ernsting, N. P. *J. Chem. Phys.*, **1995**, *102*, 2691. Nibbering, E. T. J.; Wiersma, D. A.; Duppen, K. *Chem. Phys*. **1994**, *183*, 167.

(27) Yan, Y. J.; Mukamel, S. *J. Chem. Phys*. **1988**, *89*, 5160. Yan, Y. J.; Mukamel, S. *Phys. Rev. A* **1990**, *41*, 6485. Fried, L. E.; Bernstein, N.; Mukamel, S. *Phys. Rev. Lett.* **1992**, *68*, 1842.

(28) Carter, E. A.; Hynes, J. T. *J. Chem. Phys.* **1991**, *94*, 5961. Ando, K.; Kato, S. *J. Chem. Phys.* **1991**, *95*, 5966. Fonseca, T.; Ladanyi, B. M. *J. Phys. Chem.* **1991**, *95*, 2116. Neria, E.; Nitzan, A. *J. Chem. Phys.* **1992**, *96*, 5433. Bruehl, M.; Hynes, J. T. *J. Phys. Chem.* **1992**, *96*, 4068. Maroncelli, M.; Kumar, V. P.; Papazyan, A. *J. Phys. Chem*. **1993**, *97*, 13. Cho, M.; Rosenthal, S. J.; Scherer, N. F.; Ziegler, L. D.; Fleming, G. R. *J. Chem. Phys.* **1992**, *96*, 5033.

(29) Brown, R. J. *Chem. Phys*. **1995**, *102*, 9059; private communication.

(30) Bultmann, T.; Kemeter, K.; Rusbüldt, Ch.; Bopp, P. In *Reaction Dynamics in Clusters and Condensed Phases*; Jortner, J., et al., Eds.; Kluwer: Dordrecht, 1994; p 383.

(31) Taylor, A. J.; Erskine, D. J.; Tang, C. L. *Chem. Phys. Lett.* **1984**, *103*, 5. Mokhtari, A.; Chebira, A.; Chesnoy, J. *J. Opt. Soc. Am. B* **1990**, *7*, 1551.

(32) Kang, T. J.; Jarzeba, W.; Barbara, P. F.; Fonseca, T. *Chem. Phys.* **1990**, *149*, 81. Tominaga, K.; Walker, G. C.; Jarzeba, W.; Barbara, P. F. *J. Phys. Chem.* **1991**, *95*, 10475. Tominaga, K.; Walker, G. C.; Kang, T. J.; Barbara, P. F.; Fonseca, T. *J. Phys. Chem.* **1991**, *95*, 10485.

(33) Marcus, R. A. *J. Phys. Chem.* **1989**, *93*, 3078. Kakitani, T.; Mataga, N. *J. Phys. Chem.* **1987**, *91*, 6277. Hatano, Y.; Saito, M.; Kakitani, T.; Mataga, N. *J. Phys. Chem*. **1988**, *92*, 1008.

(34) King, G.; Warshel, A. *J. Chem. Phys.* **1990**, *93*, 8682. Papazyan, A.; Maroncelli, M. *J. Chem. Phys.* **1991**, *95*, 9219. Carter, E. A.; Hynes, J. T. *J. Phys. Chem.* **1989**, *93*, 2184. Fonseca, T.; Ladanyi, B. M.; Hynes, J. T. *J. Phys. Chem.* **1992**, *96*, 4085. Yoshimori, A.; Kakitani, T.; Enomoto, Y.; Mataga, N. *J. Phys. Chem.* **1989**, *93*, 8316.

(35) Tachiya, M. *Chem. Phys. Lett.* **1989**, *159*, 505. Tachija, M. *J. Phys. Chem*. **1989**, *93*, 7050. Weintraub, O.; Bixon, M. *J. Phys. Chem.* **1994**, *98*, 3407. Calef, B. F.; Wolynes, P. G. *J. Chem. Phys.* **1983**, *78*, 470.

(36) Van der Meulen, P.; Zhang, H.; Glasbeek, M. To be published.

(37) Walker, G. C.; Akesson, E.; Johnson, A. E.; Levinger, N. E.; Barbara, P. F. *J. Phys. Chem.* **1992**, *96*, 3728. Reid, P. J.; Barbara, P. F. *J. Phys. Chem.* **1995**, *99*, 3554. Tominaga, K.; Kliner, D. A. V.; Johnson, A. E.; Levinger, N. E.; Barbara, P. F. *J. Chem. Phys.* **1993**, *98*, 1228. Reid, P. J.; Silva, C.; Barbara, P. F.; Karki, L.; Hupp, J. T. *J. Phys. Chem.* **1995**, *99*, 2609.

(38) Nagasawa, Y.; Yartsev, A. P.; Tominaga, K.; Johnson, A. E.; Yoshihara, K. *J. Chem. Phys.* **1994**, *101*, 5717.

(39) Kobayashi, T.; Takagi, Y.; Kandori, H.; Kemnitz, K.; Yoshihara, K. *Chem. Phys. Lett.* **1991**, *180*, 416.

(40) Rips, I.; Jortner, J. *J. Chem. Phys.* **1987**, *87*, 2090. Jortner, J.; Bixon, M. *J. Chem. Phys.* **1988**, *88*, 167. Bixon, M.; Jortner, J. *Chem. Phys.* **1993**, *176*, 467.

JP952949R